Probing Higgs couplings at LHC and beyond

Biplob Bhattacherjee*
Centre for High Energy Physics Indian Institute of Science 560012 Bangalore, India

Tanmoy Modak,† Sunando Kumar Patra,‡ and Rahul Sinha§
The Institute of Mathematical Sciences, Taramani, Chennai 600113, India

The study of the Higgs couplings following its discovery is the priority of future LHC runs. A hint of anomalous nature will be exhibited via its coupling to the Standard Model(SM) particles and open up new domain of phenomenological study of physics beyond the Standard Model. The enhanced statistics from next LHC runs will enable entry into the precision era to study the properties of Higgs with greater details. In this paper we present how one can extract Higgs couplings in future LHC runs at 14 TeV via $H \to ZZ^* \to 4\ell$, using observables constructed from angular distributions for the Standard Model Higgs and Higgs with mixed CP configuration. We show how angular asymmetries can be used to measure the ratios of the couplings and the relative phases at LHC. We benchmark our analysis finding out the angular asymmetries and the best fit values of the ratios of the couplings for SM Higgs, CP-odd admixture, CP-even higher derivative contribution and when CP-even higher derivative contribution and CP-odd admixture are both present. In the Standard Model, HZZ couplings have no momentum dependence. It is thus essential to demonstrate the momentum independence of the couplings to establish the couplings are SM like in nature. In this work we show how one can test the momentum independence of the Standard Model like coupling using angular asymmetries. We develop the necessary tools and demonstrate how to study the momentum dependence can be studied at future LHC runs.

I. INTRODUCTION

The ATLAS [1, 2] and CMS [3–5] collaboration at LHC have both discovered a new resonance of mass around 125 GeV that is found to be largely consistent with the observation of a Higgs boson. Several studies [6–59] done both before and after the discovery of the Higgs boson have examined how to determine the spin, parity and coupling of the Higgs boson. In gauge sector, decay modes such as $H \to \gamma\gamma$, $H \to ZZ$ and $H \to WW$ etc., where one (or both) of the Z's and W's are off-shell, are used to study the spin, parity and coupling of the Higgs boson. Observation of the decay mode $H \to \gamma\gamma$ establishes that the discovered resonance is necessarily a boson and the Landau-Yang theorem [65, 66] excludes the possibility of it having spin $J = 1$. Furthermore if Higgs boson is a eigenstate of charge conjugation, charge conjugation invariance along with observation of $H \to \gamma\gamma$ also enforce [10] that Higgs is a charge conjugation $C = +$ state. Recent measurements [70–73] have shown that the resonance favors Spin 0 over spin 2. Moreover Ref.[55] rules out pure pseudoscalar hypothesis i.e. $J^P = 0^-$ at a 99.98 % CL. However the discovered Higgs can still have small CP-odd admixture or higher derivative CP-even contribution to its coupling. Angular distributions and angular asymmetries of Higgs decay are essential to investigate whether the discovered resonance is a CP eigenstate or a resonance with mixed CP configuration. As these angular asymmetries are functions of the Higgs couplings, studying them will allow us to probe the nature of the Higgs coupling directly.

In this paper we will restrict ourselves to experimentally clean golden channel $H \to ZZ^* \to (\ell_1^-\ell_1^+)(\ell_2^-\ell_2^+)$, where ℓ_1, ℓ_2 are leptons e or μ. We consider Spin-0 Higgs boson H with even parity but, include the possibility of a small CP-odd admixture and higher derivative CP-even contribution. We first calculate the differential decay rate for $H \to ZZ^* \to (\ell_1^-\ell_1^+)(\ell_2^-\ell_2^+)$ process in terms of invariant mass of the dileptons coming from the off shell Z boson and angular distributions of the final state leptons. From these distributions, we construct angular asymmetries (observables) and utilize them to probe anomaly in HZZ couplings. Similar asymmetries have also been discussed in Ref .[60–62]. As these observables are functions of HZZ vertex factors, the values of the different observables differ for the various cases such as SM Higgs, CP-odd admixture, CP-even higher derivative contribution. Ref.[53, 55] have discussed how ratios of couplings can be measured at 8 TeV LHC run. Ref.[53] shows how using uniangular distribution as input in likelihood analysis one can discriminate different spin possibilities. In this paper a study showing how using simple angular asymmetries one can study the CP property of H in future LHC runs.

We benchmark these observables for SM Higgs and Higgs with a CP-odd admixture at 14 TeV 300 fb^{-1} LHC. We determine the ratios of the coupling constants and use them to discriminate possible CP-odd admixture from SM Higgs. We then perform the same analysis at 3000 fb^{-1} to distinguish SM, case with CP-odd admixture and CP-even higher derivative contribution. We also consider the scenario when higher derivative CP-even and and CP-

* biplobcts@iisc.ernet.in
† tanmoyy@imsc.res.in
‡ sunandokp@imsc.res.in
§ sinha@imsc.res.in

odd admixture are present in HZZ couplings. We denote this scenario as 'CP-even-odd' case. In our analysis we have also included a complex phase for CP-odd admixture Higgs and show how to determine the phase using angular asymmetries. Furthermore we use these angular asymmetries and perform chi-square analysis to probe both CP-even and CP-odd anomalous contributions in the Higgs couplings.

Exotic models of Higgs can have momentum dependence in its couplings. It is thus essential to study the momentum dependence of the Higgs couplings to establish its SM nature. Angular asymmetries will provide necessary tools to investigate the momentum dependence of the Higgs couplings. In our work we develop necessary techniques and utilize them to probe the momentum dependence of HZZ couplings. It is important to note this it will definitely require higher statistics. However the enhanced statistics at 14 TeV, LHC will enable us to study the momentum dependence of Higgs couplings in different momentum regions. Since the mass of H does not allow both the Z bosons to be on-shell, the invariant mass distribution of the dileptons from the off-shell Z boson(Z_2) will offer us a test for the momentum dependence of the HZZ couplings. The HZZ couplings in the most general case could be function of the invariant mass of the off-shell Z. The constancy of the ratios of the Higgs couplings can be measured by finding out the values of the ratios of couplings in different momentum regions for the invariant mass of the off-shell Z. In our analysis we have shown for SM how one can test the momentum dependence of the Higgs couplings at 14 TeV 300 fb^{-1} LHC run.

In LHC we measure $\sigma \cdot BR$ and that does not allow us to measure the decay width of the Higgs, as a result we can only measure the ratios of Higgs couplings. However ILC[63] will be able to measure the inclusive cross section(σ_{ZH}) using recoil technique for the process $e^+e^- \to ZH$. Hence inclusive cross section provide a direct measurement of HZZ couplings at ILC by measuring partial width $\Gamma(H \to ZZ)$. After energy upgrade LHC will run at 33 TeV and enhanced statistics will enable us to measure Higgs couplings more precisely than that possible at 14 TeV. We discuss how much this energy upgrade will improve the measurement of HZZ couplings and discuss what sensitivity can be achieved compared to that of an ILC[64] measurement.

The paper is organized as follows: In Section II we formalize the necessary tools for our analysis. Section III is divided into three subsection. First we benchmark our analysis for 300 fb^{-1} in Subsection III A and then we benchmark our analysis for 3000 fb^{-1} for SM Higgs, Higgs with CP-odd admixture, CP-even higher derivative contribution and CP-even-odd scenario in Subsection III B. In Subsection III C we develop the necessary technique to measure the momentum dependence of Higgs couplings. A qualitative comparison between future runs of LHC and ILC precision measurement has been made in Section IV. Finally we conclude in Section V.

II. THE FORMALISM

In this section we first write down the HZZ vertex, helicity amplitudes in transversity basis and finally derive the expression for angular distribution of $H \to ZZ^* \to 4\ell$ process assuming H to be a spin 0 particle. In SM the process $H \to ZZ$ is characterised by the Lagrangian

$$\mathcal{L}_{HZZ} = \frac{gM_Z}{2\cos\theta_W} Z_\mu Z^\mu H \tag{1}$$

where θ_W is the Weinberg angle and g is the electroweak coupling constant. However there may exist anomalous couplings of H to Z boson. These couplings can in general be CP-even or CP-odd and can be generated from the effective Lagrangians

$$\mathcal{L}_e \sim -\frac{1}{4} Z^{\mu\nu} Z_{\mu\nu} H \tag{2}$$

and

$$\mathcal{L}_o \sim -\frac{1}{4} Z^{\mu\nu} \tilde{Z}_{\mu\nu} H \tag{3}$$

respectively, where $Z_{\mu\nu}$ and $\tilde{Z}_{\mu\nu}$ are defined as $Z_{\mu\nu} = \partial_\mu Z_\nu - \partial_\nu Z_\mu$ and $\tilde{Z}_{\mu\nu} = \epsilon_{\mu\nu\rho\sigma} Z^{\rho\sigma}$ respectively.

Following these Lagrangians one can write down the most general HZZ vertex as follows

$$V^{\mu\nu} = \frac{igM_Z}{\cos\theta_W}\Big(a\, g^{\mu\nu} + b\, (q_2^\mu q_1^\nu - q_1\cdot q_2\, g^{\mu\nu}) + ic\,\epsilon^{\mu\nu\rho\sigma}\, q_{1\rho}\, q_{2\sigma}\Big), \tag{4}$$

where a, b, c are momentum dependent vertex factors and q_1, q_2 and P are the four momenta of $Z(Z_1)$, $Z^*(Z_2)$ and H respectively. Off-shellness of the Z is denoted by the superscript '*'. In Standard Model at tree level the values of the vertex factors are $a = 1$ and $b = c = 0$ and they are constant. However a non zero b and c can arise from higher order correction. If the vertex factors a, b, c show any deviations from SM values or exhibit a momentum dependence it would provide a hint about the non standard nature of the HZZ couplings. The CP-ood admixture is charactersided by the non zero value of c of the form $c\, e^{i\delta}$, where δ is the CP violating phase associated with c.

The decay under consideration can be characterised by three helicity amplitudes $\mathcal{A}_L$, $\mathcal{A}_\parallel$ and $\mathcal{A}_\perp$ defined as (see appendix) :

$$\mathcal{A}_L = q_1\cdot q_2\, (a - b\, q_1.q_2) + M_H^2\, X^2\, b, \tag{5}$$

$$\mathcal{A}_\parallel = \sqrt{2q_1^2\, q_2^2}\, (a - b\, q_1.q_2)\,, \tag{6}$$

$$\mathcal{A}_\perp = \sqrt{2q_1^2\, q_2^2}\, X\, M_H\, c, \tag{7}$$

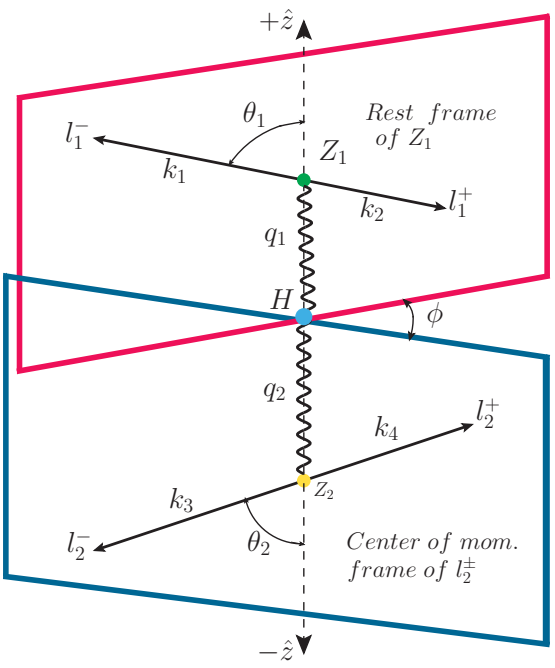

FIG. 1. The definition of the polar angles (θ_1 and θ_2) and the azimuthal angle (ϕ) in the decay of Higgs (H) to a pair of Z boson, followed by a decay of both the Z into four charged leptons: $H \to Z_1 + Z_2 \to (\ell_1^- + \ell_1^+) + (\ell_2^- + \ell_2^+)$, where $\ell_1, \ell_2 \in \{e, \mu\}$ and three momentum $\vec{k}_1 = -\vec{k}_2$ and $\vec{k}_3 = -\vec{k}_4$.The lepton pair $\ell_1^\pm$ going back to back in the rest frame of Z_1, however lepton pair from Z_2 going back to back in their center-of-momentum (C.O.M) frame.

where $\sqrt{q_1^2}$ and $\sqrt{q_2^2}$ are the invariant masses of the Z_1 and Z_2 respectively, with

$$X = \frac{\sqrt{\lambda(M_H^2, q_1^2, q_2^2)}}{2M_H}, \tag{8}$$

and

$$\lambda(x, y, z) = x^2 + y^2 + z^2 - 2\,x\,y - 2\,x\,z - 2\,y\,z\ . \tag{9}$$

The helicity amplitudes have definite parity properties as $\mathcal{A}_L$, $\mathcal{A}_\parallel$ are CP-even and $\mathcal{A}_\perp$ is CP-odd.

Having defined the helicity amplitudes in transversity basis the full angular distribution for $H \to Z_1 + Z_2 \to (\ell_1^- + \ell_1^+) + (\ell_2^- + \ell_2^+)$, can be written as[53]

$$\begin{aligned}
\frac{8\pi}{\Gamma_{\rm f}}\frac{d^4\Gamma}{dq_2^2\, d\cos\theta_1\, d\cos\theta_2\, d\phi} &= 1 + \frac{|\mathcal{F}_\parallel|^2 - |\mathcal{F}_\perp|^2}{4}\cos 2\phi\big(1 - P_2(\cos\theta_1)\big)\big(1 - P_2(\cos\theta_2)\big) + \frac{1}{2}\mathrm{Im}(\mathcal{F}_\parallel\mathcal{F}_\perp^*)\sin 2\phi \\
&\times \big(1 - P_2(\cos\theta_1)\big)\big(1 - P_2(\cos\theta_2)\big) + \frac{1}{2}(1 - 3\,|\mathcal{F}_L|^2)\,\big(P_2(\cos\theta_1) + P_2(\cos\theta_2)\big) + \frac{1}{4}(1 + 3\,|\mathcal{F}_L|^2)\,P_2(\cos\theta_1)P_2(\cos\theta_2) \\
&+ \frac{9}{8\sqrt{2}}\Big(\mathrm{Re}(\mathcal{F}_L\mathcal{F}_\parallel^*)\,\cos\phi + \mathrm{Im}(\mathcal{F}_L\mathcal{F}_\perp^*)\,\sin\phi\Big)\sin 2\theta_1\,\sin 2\theta_2\ + \eta\frac{9}{2\sqrt{2}}\mathrm{Re}(\mathcal{F}_L\mathcal{F}_\perp^*)\big(\cos\theta_1 - \cos\theta_2\big)\cos\phi\sin\theta_1\sin\theta_2 \\
&+ \eta\frac{3}{2}\mathrm{Re}(\mathcal{F}_\parallel\mathcal{F}_\perp^*)\big(\cos\theta_2(2 + P_2(\cos\theta_1)) - \cos\theta_1(2 + P_2(\cos\theta_2))\big) - \eta\frac{9}{2\sqrt{2}}\mathrm{Im}(\mathcal{F}_L\mathcal{F}_\parallel^*)\big(\cos\theta_1 - \cos\theta_2\big)\sin\phi\sin\theta_1\sin\theta_2 \\
&- \frac{9}{4}\eta^2\left((1 - |\mathcal{F}_L|^2)\cos\theta_1\cos\theta_2 + \sqrt{2}\,\Big(\mathrm{Re}(\mathcal{F}_L\mathcal{F}_\parallel^*)\cos\phi + \mathrm{Im}(\mathcal{F}_L\mathcal{F}_\perp^*)\sin\phi\Big)\sin\theta_1\sin\theta_2\right),
\end{aligned} \tag{10}$$

where $\mathcal{F}_L$, $\mathcal{F}_\parallel$, $\mathcal{F}_\perp$ are the *helicity fractions* defined in the appendix along with $\Gamma_{\rm f}$ and η. The angle $\theta_1(\theta_2)$ is the angle between three momenta of ℓ_1^- (ℓ_2^-) in $Z_1(Z_2)$ rest frame and the direction of three momenta of $Z_1(Z_2)$ in H rest frame. The angle ϕ is defined as the angle between the normals to the planes defined by $Z_1 \to \ell_1^-\ell_1^+$ and $Z_2 \to \ell_2^-\ell_2^+$ in H rest frame as shown in Fig. 1. It should be noted that Eq.(10) is *exact* and *no assumptions has been made apart from assuming that the leptons are massless.*

Integrating Eq.(10) with respect to any two out of the three angles θ_1, θ_2, ϕ one finds three uniangular distributions for the process $H \to ZZ \to (\ell_1^-\ell_1^+)(\ell_2^-\ell_2^+)$ as:

$$\frac{1}{\Gamma_{\rm f}}\frac{d^2\Gamma}{dq_2^2\, d\cos\theta_1} = \frac{1}{2} + T_2\,P_2(\cos\theta_1) - T_1\cos\theta_1, \tag{11}$$

$$\frac{1}{\Gamma_{\rm f}}\frac{d^2\Gamma}{dq_2^2\, d\cos\theta_2} = \frac{1}{2} + T_2\,P_2(\cos\theta_2) + T_1\cos\theta_2, \tag{12}$$

$$\frac{2\pi}{\Gamma_f}\frac{d^2\Gamma}{dq_2^2\, d\phi} = 1 + U_2\cos 2\phi + V_2\sin 2\phi + U_1\cos\phi + V_1\sin\phi, \quad (13)$$

The observables T_1, T_2, U_1, U_2, V_1 and V_2 are defined as:

$$T_1 = \frac{3}{2}\eta \mathrm{Re}(\mathcal{F}_\parallel \mathcal{F}_\perp^*), \quad (14)$$

$$T_2 = \frac{1}{4}(1 - 3\,|\mathcal{F}_L|^2), \quad (15)$$

$$U_1 = -\frac{9\pi^2}{32\sqrt{2}}\eta^2\,\mathrm{Re}(\mathcal{F}_L \mathcal{F}_\parallel^*), \quad (16)$$

$$U_2 = \frac{1}{4}(|\mathcal{F}_\parallel|^2 - |\mathcal{F}_\perp|^2), \quad (17)$$

$$V_1 = -\frac{9\pi^2}{32\sqrt{2}}\eta^2\,\mathrm{Im}(\mathcal{F}_L \mathcal{F}_\perp^*), \quad (18)$$

$$V_2 = \frac{1}{2}\,\mathrm{Im}(\mathcal{F}_\parallel \mathcal{F}_\perp^*), \quad (19)$$

and are functions of q_2^2. Moreover $P_1(\cos\theta_{1,2})$ $P_2(\cos\theta_{1,2})$ are first and second degree Legendre Polynomials respectively. It should be noted that the observables T_1, T_2, U_1, U_2, V_1 and V_2 are coefficients of orthogonal functions $P_2(\cos\theta_{1,2})$, $P_1(\cos\theta_{1,2})$, $\cos 2\phi$, $\cos\phi$, $\sin 2\phi$, $\sin\phi$ respectively and can be extracted individually. These observables are functions of the helicity fractions $\mathcal{F}_L$, $\mathcal{F}_\parallel$ and $\mathcal{F}_\perp$, hence they are functions of vertex factors a, b and c. Measurement of these observables will enable us to probe the vertex factors a, b and c. Moreover in SM T_2, U_2 and U_1 all are non zero as $\mathcal{F}_L$ and $\mathcal{F}_\parallel$ are non zero. In SM at tree level $c = 0$ which enforces $\mathcal{F}_\perp = 0$. As T_1, V_2 and V_1 all are functions of $\mathcal{F}_\perp = 0$, in SM they are all zero. A CP-odd admixture is characterised by non zero value of c and hence non vanishing values of T_1, V_2 and V_1. Measurements of T_1, V_2 and V_1 allow us to probe CP violating phase in HZZ couplings. If there exist any CP-even higher derivative contribution in HZZ couplings, the vertex factor b becomes non zero, hence the observables T_2, U_2 and U_1 will have different values than that of SM. In SM at tree level $b = 0$ but at one loop level the value of b will be non zero. Measurement of b will allow us to probe triple-Higgs vertex which arises at one loop level and provide the first verification of Higgs self coupling.

This observables can be extracted using following angular asymmetries

$$T_1 = \left(\int_{-1}^{0} - \int_{0}^{+1}\right) d\cos\theta_1 \left(\frac{1}{\Gamma_f}\frac{d^2\Gamma}{dq_2^2\, d\cos\theta_1}\right) = \left(-\int_{-1}^{0} + \int_{0}^{+1}\right) d\cos\theta_2 \left(\frac{1}{\Gamma_f}\frac{d^2\Gamma}{dq_2^2\, d\cos\theta_2}\right), \quad (20)$$

$$T_2 = \frac{4}{3}\left(\int_{-1}^{-\frac{1}{2}} - \int_{-\frac{1}{2}}^{+\frac{1}{2}} + \int_{+\frac{1}{2}}^{+1}\right) d\cos\theta_{1,2} \left(\frac{1}{\Gamma_f}\frac{d^2\Gamma}{dq_2^2\, d\cos\theta_{1,2}}\right), \quad (21)$$

$$U_1 = \frac{1}{4}\left(-\int_{-\pi}^{-\frac{\pi}{2}} + \int_{-\frac{\pi}{2}}^{+\frac{\pi}{2}} - \int_{+\frac{\pi}{2}}^{+\pi}\right) d\phi \left(\frac{2\pi}{\Gamma_f}\frac{d^2\Gamma}{dq_2^2\, d\phi}\right), \quad (22)$$

$$U_2 = \frac{\pi}{2\Gamma_f}\left(\int_{-\pi}^{-\frac{3\pi}{4}} - \int_{-\frac{3\pi}{4}}^{-\frac{\pi}{4}} + \int_{-\frac{\pi}{4}}^{\frac{\pi}{4}} - \int_{\frac{\pi}{4}}^{\frac{3\pi}{4}} + \int_{\frac{3\pi}{4}}^{\pi}\right) d\phi\, \frac{d^2\Gamma}{dq_2^2\, d\phi}, \quad (23)$$

$$V_1 = \frac{1}{4}\left(-\int_{-\pi}^{0} + \int_{0}^{+\pi}\right) d\phi \left(\frac{2\pi}{\Gamma_f}\frac{d^2\Gamma}{dq_2^2\, d\phi}\right), \quad (24)$$

$$V_2 = \frac{1}{4}\left(\int_{-\pi}^{-\frac{\pi}{2}} - \int_{-\frac{\pi}{2}}^{0} + \int_{0}^{+\frac{\pi}{2}} - \int_{+\frac{\pi}{2}}^{+\pi}\right) d\phi \left(\frac{2\pi}{\Gamma_f}\frac{d^2\Gamma}{dq_2^2\, d\phi}\right). \quad (25)$$

Three uniangular distributions in Eq.(11), Eq.(12) and Eq.(13) give 6 observables T_1, T_2, U_1, V_1 and V_2 in terms of angular asymmetries shown above. At 14 TeV, high luminosity future LHC runs will provide enhanced statistics and the uniangular distributions will not only allow us to probe Higgs couplings, but also provide us with arsenal to probe the momentum dependence of the Higgs couplings which is essential for precision measurement. In the next section we will discuss these aspects in detail.

III. NUMERICAL STUDY

In this section we demonstrate how angular analysis can be used to benchmark different CP scenarios of H. We have generated events with MADEVENT5 [75] event generator interfaced with PYTHIA6.4 [76] and Delphes 3 [77]. The vertex, Eq. (4) is parametrized by UFO format of MadGraph5 using HiggsCharacterisation model [78]. The events are generated by pp collisions via $gg \to H$ and $gg \to H + 1jet$, for center of mass en-

ergy $\sqrt{s} = 14$ TeV, using parton distribution functions CTEQ6L1 [74].

For matching purpose we have used MLM prescription and events are finally passed through fast detector simulator package Delphes 3. We are only concerned about the decay process of the H and have assumed only the SM production process of H while generating events.

We follow the cut based analysis of Ref.[73]. The identical pairs of final state leptons $2e^+2e^-$ and $2\mu^+2\mu-$ events have also been taken into account for our analyses. The on-shell Z_1 boson is identified by the invariant mass of the opposite charge same flavor lepton pairs closest to M_Z. Moreover, since the Higgs mass M_H does not allow both the Z bosons to be on-shell, this in turn breaks the need for Fermi antisymmetrisation of the identical fermions when the final states are $2e^+2e^-$ and $2\mu^+2\mu-$. The branching ratios and cross sections have been taken from Higgs working Group webpage [79].

Following the analysis presented in Ref.[73] data are selected using single-lepton or di-lepton triggers. For the single-muon trigger the transverse momentum, P_T, threshold is 25 GeV, while for single-electron trigger the transverse energy, E_T, threshold is 25 GeV. Di-muon triggers are selected using two ways. For asymmetric di-muon the trigger thresholds are either $p_{T1} = 18$ GeV and $p_{T2} = 8$ GeV. Threshold for symmetric di-muon triggers are $p_T = 13$ GeV for both the muons. For the di-electron trigger the thresholds are $E_T = 12$ GeV for both electrons. There are two electron-muon triggers used with 12 or 24 GeV E_T electron thresholds, differed by the electron identification requirements, and muon threshold $p_T = 8$ GeV.

Each electron (muon) must satisfy $E_T > 7$ GeV ($p_T > 6$ GeV) and be measured in the pseudo-rapidity range $|\eta| < 2.47$ ($|\eta| < 2.7$). We have selected the leptons in two sequential p_T ordered way.
i) Case-I : p_T of at least two leptons in a quadruplet must satisfy $p_T > 20$ GeV,
ii) Case-II : p_T of at least three leptons in a quadruplet must satisfy $p_T > 20$ GeV.

The leptons are required to be separated from each other by $\Delta R > 0.1$ if they are of the same flavour and $\Delta R > 0.2$ otherwise. Each event is required to have the triggering lepton(s) correctly matched to one or two of the selected leptons.

Furthermore we also impose the invariant mass cuts on the $m_{Z_1}(\sqrt{q_1^2})$, $m_{Z_2}(\sqrt{q_2^2})$ and $m_{4\ell}$ described in Table I. m_{Z_1} is the invariant mass of the pair of opposite sign same flavor leptons closest to m_Z while m_{Z_2} is the other combination. The two columns of Table I demonstrate the effect of p_T ordering in event selection.

Now integrating Eq. (11),(12), (13) over q_2^2 we get three integrated distributions as follows

$$\frac{1}{\Gamma}\frac{d\Gamma}{d\cos\theta_1} = \frac{1}{2} - \mathcal{T}_1\,\cos\theta_1 + \mathcal{T}_2\,P_2(\cos\theta_1), \qquad (26)$$

Cuts	Case-I	Case-II
Selection cuts	494	2253
50 GeV $< m_{12} <$ 106 GeV	487	2204
12 GeV $< m_{34} <$ 115 GeV	447	2071
115 GeV $< m_{4\ell} <$ 130 GeV	443	2050

TABLE I. Effects of the sequential cuts on the simulated Signal for two different p_T ordering of Case-I(first column) and Case-II(second column). The sequential p_T ordering of Case-I is for 300 fb^{-1}, however we have used sequential p_T ordering of Case-II for 3000 fb^{-1}. The k-factor for signal is 2.5.

$$\frac{1}{\Gamma}\frac{d\Gamma}{d\cos\theta_2} = \frac{1}{2} + \mathcal{T}_1\,\cos\theta_2 + \mathcal{T}_2\,P_2(\cos\theta_2), \qquad (27)$$

$$\frac{1}{\Gamma}\frac{d\Gamma}{d\phi} = \frac{1}{2\pi} + \mathcal{U}_1\,\cos\phi + \mathcal{U}_2\,\cos 2\phi + \mathcal{V}_1\,\sin\phi + \mathcal{V}_2\,\sin 2\phi, \qquad (28)$$

where $\mathcal{T}_1$, $\mathcal{T}_2$, $\mathcal{U}_1$, $\mathcal{U}_2$, $\mathcal{V}_1$ and $\mathcal{V}_2$ are observables integrated over $m_{34}(q_2^2)$ and m_{12}.

The normalized distributions, $\frac{1}{\Gamma}\frac{d\Gamma}{d\cos\theta_1}$ vs $\cos\theta_1$, $\frac{1}{\Gamma}\frac{d\Gamma}{d\cos\theta_2}$ vs $\cos\theta_2$ and $\frac{1}{\Gamma}\frac{d\Gamma}{d\phi}$ vs ϕ for SM are shown in Fig. 2, Fig. 3 and Fig. 4 respectively for simulated data. It should be noted that the angular coverage for $\cos\theta_1$ or $\cos\theta_2$ covers the full range from -1 to $+1$ and coverage for ϕ from 0 to 2π are still retained even after using actual detector scenarios. The cut flow analysis of Case-I is followed for the analysis of SM Higgs and Higgs with CP-odd admixture at 300 fb^{-1}. At 3000 fb^{-1} since the statistics is higher, we will use stronger cut based analysis i.e. sequential cut flow analysis of Case-II for benchmarking SM Higgs and Higgs with different CP configuration. Moreover it should be noted that we have used the same cut based analysis for CP-odd admixture, CP-even higher derivative contribution and CP-even-odd scenario. The cross section for each benchmark scenarios are within the current experimental allowed region.

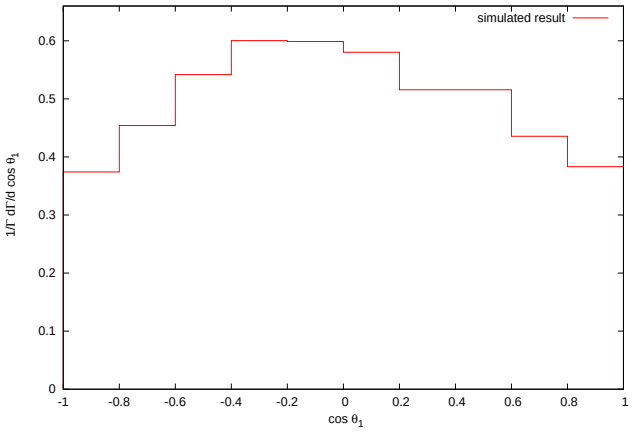

FIG. 2. The normalized distribution $\frac{1}{\Gamma}\frac{d\Gamma}{d\cos\theta_1}$ vs $\cos\theta_1$ for SM Higgs events.

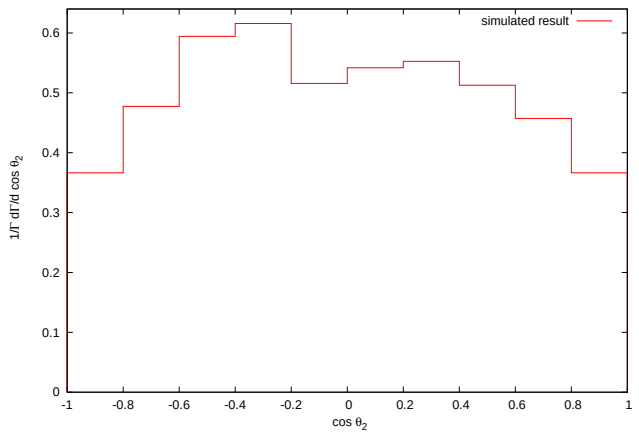

FIG. 3. The normalized distribution $\frac{1}{\Gamma}\frac{d\Gamma}{d\cos\theta_2}$ vs $\cos\theta_2$ for SM Higgs events.

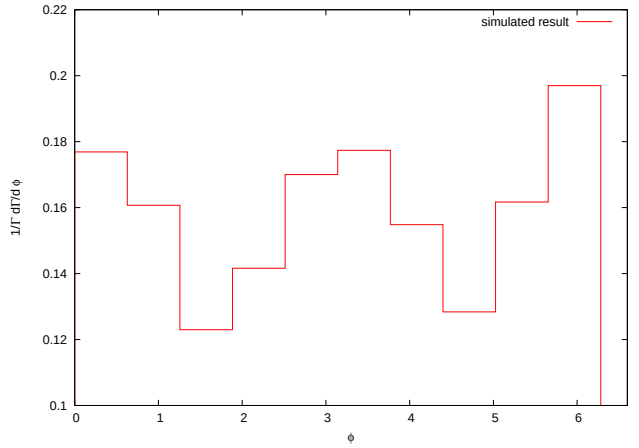

FIG. 4. The normalized distribution $\frac{1}{\Gamma}\frac{d\Gamma}{d\phi}$ vs ϕ for SM Higgs events.

The simulated data are binned in $\cos\theta_1$, $\cos\theta_2$ and ϕ and fitted using Eq.(26), Eq.(27) and Eq.(28) to obtain the angular asymmetries t_1, t_2, u_1, u_2, v_1, v_2 and their errors which correspond to the angular asymmetries $\mathcal{T}_1$, $\mathcal{T}_2$, $\mathcal{U}_1$, $\mathcal{U}_2$, $\mathcal{V}_1$ and $\mathcal{V}_2$ respectively. Once the values of the integrated observables t_1, t_2, u_1, u_2, v_1, v_2 and their respective errors are found, the χ^2 formula:

$$\chi^2 = \frac{(\mathcal{T}_2 - t_2)^2}{(\Delta t_2)^2} + \frac{(\cos\delta\,\mathcal{T}_1 - t_1)^2}{(\Delta t_1)^2} + \frac{(\mathcal{U}_1 - u_1)^2}{(\Delta u_1)^2} + \frac{(\mathcal{U}_2 - u_2)^2}{(\Delta u_2)^2} + \frac{(\sin\delta\,\mathcal{V}_2 - v_2)^2}{(\Delta v_2)^2} + \frac{(\sin\delta\,\mathcal{V}_1 - v_1)^2}{(\Delta v_1)^2} \tag{29}$$

will find the b/a, c/a and the phase δ. The errors in b/a, c/a and phase δ can also be calculated using the error matrix

$$\left(\frac{\partial^2\chi^2}{\partial\alpha_i\partial\alpha_i}\right)_{\hat{\alpha}} \tag{30}$$

where $\alpha_i, \alpha_j = b/a, c/a, \delta$. To find the best fit values we have used Mathematica 9[69].

A. Study of angular asymmetries of Higgs at 14 TeV and 300 fb^{-1}

We start benchmarking angular observables for SM Higgs and Higgs with CP-odd admixture in this section. The fit values for observables are tabulated along with the best fit values of b/a, c/a and phase δ of the CP-odd coupling. We also obtain 1σ and 2σ contours for b/a vs c/a and δ vs c/a for the case of CP-odd admixture. This will provide the precision at which one can rule out anomalous contributions in HZZ couplings, establishing the SM nature of H at 14 TeV 300 fb^{-1} LHC run.

1. *SM Higgs*

SM Higgs events are generated with $a = 1$, $b = 0$, $c = 0$. The fit values of the observables for the SM Higgs are tabulated in Table II.

TABLE II. The values of the observables for the SM Higgs with respective errors.

Observables	Values with errors
t_2	-0.21 ± 0.09
t_1	$(-1.6 \pm 7.16) \times 10^{-2}$
u_2	0.32 ± 0.40
u_1	$(0.93 \pm 4.36) \times 10^{-1}$
v_2	$(-0.72 \pm 4.03) \times 10^{-1}$
v_1	$(0.19 \pm 3.70) \times 10^{-1}$

The values of the observables t_2 and u_2 are large compared to other observables as discussed in the previous section, playing important role in the χ^2 expression in Eq.(29). The observables t_1, v_2 and v_1 provide information about phase for anomalous couplings b and c. The best fit values of b/a and c/a with their respective errors for the SM Higgs are given as follows:

$$b/a = (0.50 \pm 0.96) \times 10^{-4}\,\text{GeV}^{-2} \tag{31}$$

$$c/a = (0.68 \pm 2.27) \times 10^{-4}\,\text{GeV}^{-2} \tag{32}$$

The best fit values with 1σ and 2σ contours for b/a vs c/a are shown in Fig .5.

2. *Higgs with CP-odd admixture*

The CP-odd admixture is charaterised by a non zero value of c in Eq.(4). For CP-odd admixture case, Higgs events are generated using $a = 0.7$, $b = 0$ and $c = (2.2 + 2.2i) \times 10^{-4}$. The values of the observables are given in Table III.

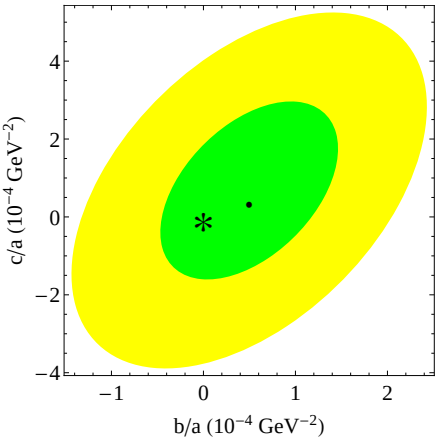

FIG. 5. c/a vs b/a 1σ (green) and 2σ (yellow) contours for the SM Higgs at 300 fb^{-1}. The best fit values $(b/a, c/a)$ is shown by the block dot. The '$*$' corresponds to $b = c = 0$.

TABLE III. The values of the observables for CP-odd admixture Higgs with respective errors at 300 fb^{-1}.

Observables	**Values with errors**
t_2	-0.06 ± 0.10
t_1	-0.11 ± 0.08
u_2	-0.08 ± 0.40
u_1	$(-0.80 \pm 4.04) \times 10^{-1}$
v_2	$(0.99 \pm 4.20) \times 10^{-1}$
v_1	$(0.44 \pm 4.21) \times 10^{-1}$

The value of t_2 has now become smaller compared to the SM case as shown in Table II. Most importantly the non zero value of t_1 arises due to the complex CP-odd anomalous coupling c. This will play a significant role along with t_2 and u_2 in probing anomalous CP-odd admixture of HZZ couplings. The best fit values for b/a, c/a and the phase δ for CP-odd admixture are :

$$b/a = (1.50 \pm 1.09) \times 10^{-4}\,\text{GeV}^{-2} \tag{33}$$

$$c/a = (5.48 \pm 1.12) \times 10^{-4}\,\text{GeV}^{-2} \tag{34}$$

$$\delta = (0.29 \pm 2.14) \text{ in radian.} \tag{35}$$

Note that the error in δ is still very large at this luminosity.

The best fit values with 1σ and 2σ contours for c/a vs b/a and δ vs c/a are shown in Fig. 6 and Fig. 7 respectively.

B. Study of angular asymmetries of Higgs at 14 TeV 3000 fb^{-1}

High Luminosity LHC (HL-LHC) i.e 14 TeV 3000 fb^{-1} run before the energy upgrade will allow us to test CP structure of HZZ couplings even more precisely. For

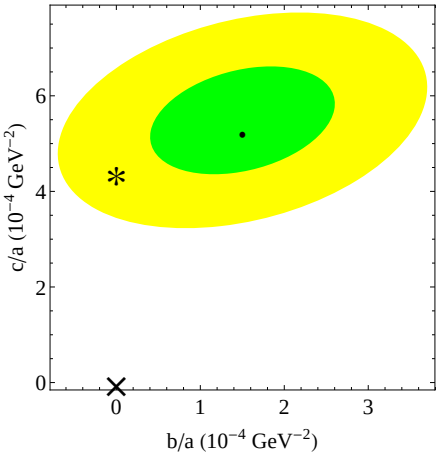

FIG. 6. c/a vs b/a 1σ (green) and 2σ (yellow) contours for CP-odd admixture Higgs at 300 fb^{-1}. The best fit value of $(b/a, c/a)$ is shown by the block dot. The values with which data are generated $(b/a = 0, c/a = 4.44 \times 10^{-4})$ is shown by the '$*$'. The cross-hair corresponds to $b = c = 0$.

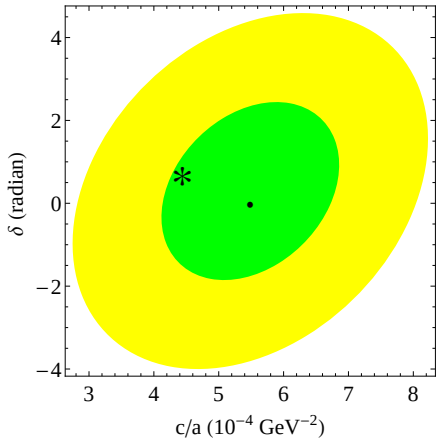

FIG. 7. δ vs c/a 1σ (green) and 2σ (yellow) contours for CP-odd admixture Higgs at 300 fb^{-1}. The best fit values $(c/a, \delta)$ is shown by the block dot. The values with which data are generated is shown by the '$*$'.

3000 fb^{-1} also, we have followed the same cut based analysis that we have discussed earlier apart from a strong sequential p_T ordering i.e. p_T of at least three leptons in a quadruplet must satisfy $p_T > 20$ GeV.

At 3000 fb^{-1} we revisit the benchmark cases of SM and CP-odd admixture along with two new analysis of CP-even higher derivative contribution and CP-even-odd scenario.

1. *SM Higgs and CP-odd admixture Higgs*

First we investigate CP-odd Higgs and SM Higgs and find out the values of angular observables along with their respective errors. For CP-odd admixture we have again taken $a = 0.7$, $b = 0$, $c = (2.2+2.2i) \times 10^{-4}$ and SM Higgs

$a = 1$, $b = 0$, $c = 0$. The fit values of the observables t_2, t_1, u_2, u_1, v_2, v_1 for the SM and CP-odd admixture Higgs are tabulated in Table IV and Table V respectively. The

TABLE IV. The values of the observables for the SM Higgs with respective errors at 3000 fb^{-1}.

Observables	Values with errors
t_2	-0.20 ± 0.04
t_1	$(0.28 \pm 0.35) \times 10^{-1}$
u_2	0.21 ± 0.19
u_1	$(0.46 \pm 2.06) \times 10^{-1}$
v_2	$(-0.07 \pm 1.96) \times 10^{-1}$
v_1	$(-0.18 \pm 1.84) \times 10^{-1}$

errors have significantly reduced for all the observables and the fit values for ratios of couplings for the SM Higgs b/a, c/a are given

$$b/a = (0.43 \pm 0.55) \times 10^{-4}\,\text{GeV}^{-2} \quad (36)$$

$$c/a = (1.08 \pm 1.17) \times 10^{-4}\,\text{GeV}^{-2} \quad (37)$$

The 1σ and 2σ contours for b/a vs c/a are shown in Fig. 8

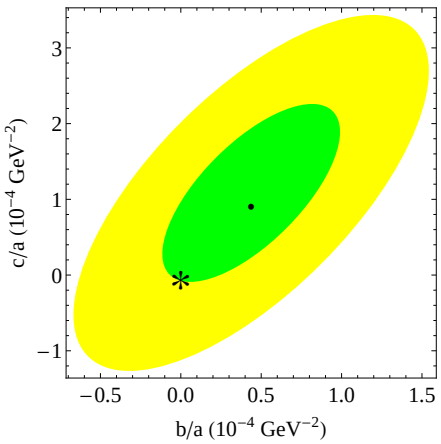

FIG. 8. c/a vs b/a 1σ (green) and 2σ (yellow) contours for the SM Higgs at 3000 fb^{-1}. The best fit values $(b/a, c/a)$ is shown by the block dot. The '$*$' corresponds to $b = c = 0$.

At 3000 fb^{-1} from Table V one can see that the errors in t_1 and t_2 are much reduced, making them very good observables for probing CP-odd admixture. The best fit values for b/a, c/a and phase δ for CP-odd admixture are given as

$$b/a = (0.40 \pm 0.54) \times 10^{-4}\,\text{GeV}^{-2} \quad (38)$$

$$c/a = (3.99 \pm 0.64) \times 10^{-4}\,\text{GeV}^{-2} \quad (39)$$

$$\delta = 0.45 \pm 1.08 \text{ in radian.} \quad (40)$$

It should be noted that the error in δ has become lower due to the fact that the error in t_1, which constraints the phase δ, is much reduced.

TABLE V. The values of the observables for CP-odd admixture Higgs with respective errors at 3000 fb^{-1}

Observables	Values with errors
t_2	-0.11 ± 0.04
t_1	-0.06 ± 0.03
u_2	0.02 ± 0.18
u_1	$(-0.10 \pm 0.56) \times 10^{-1}$
v_2	$(0.72 \pm 1.84) \times 10^{-1}$
v_1	$(0.67 \pm 1.83) \times 10^{-1}$

The 1σ and 2σ contours for b/a vs c/a and δ vs c/a are shown in Fig. 9 and Fig. 10 respectively.

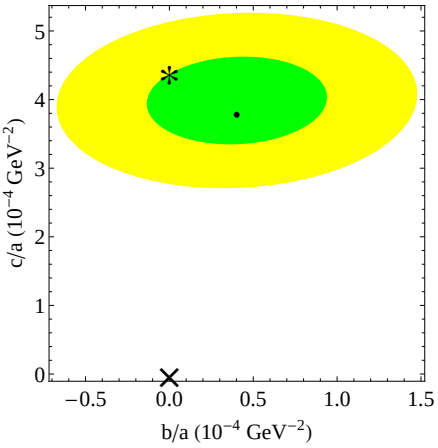

FIG. 9. c/a vs b/a 1σ (green) and 2σ (yellow) contours for CP-odd admixture Higgs at 3000 fb^{-1}. The best fit value of $(b/a, c/a)$ is shown by the block dot. The values with which data are generated $(b/a = 0, c/a = 4.44 \times 10^{-4})$ is shown by the '$*$'. The cross-hair corresponds to $b = c = 0$.

So far, we have discussed how using angular asymmetries one can probe HZZ couplings of the SM Higgs and Higgs with mixed CP scenarios at 14 TeV for two different luminosity 300 fb^{-1} and 3000 fb^{-1}. The values of the observables vary depending on the values of a, b and c. The observables T_1, V_1 and V_2 are sensitive to CP-odd admixture and can be a good candidate to probe CP-odd admixture. Finally the best fit values for the ratios of the couplings, b/a and c/a are calculated using Eq.(29).

2. *Higgs with CP-even higher derivative contribution and CP-even-odd scenario*

In this subsection we benchmark the angular asymmetries for the cases:
1)Higgs with CP-even higher derivative contribution.
2)Higgs with both CP-odd and CP-even higher derivative contribution i.e. CP-even-odd scenario.
For CP-even higher derivative contribution we have taken $a = 0.80$, $b = 10^{-4}$, $c = 0$. However for the CP-even-

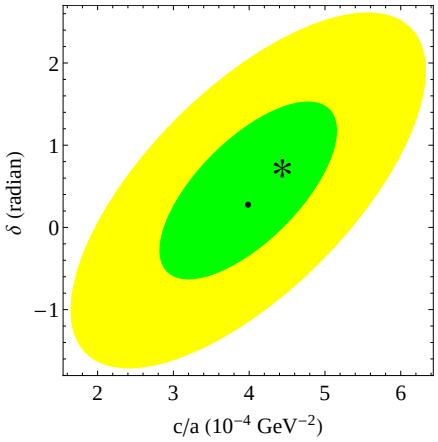

FIG. 10. δ vs c/a 1σ (green) and 2σ (yellow) contours for CP-odd admixture Higgs at 3000 fb^{-1}. The best fit values $(c/a, \delta)$ is shown by the block dot. The cross-hair corresponds to $\delta = c = 0$. The value with which data are generated is shown by the '$*$'.

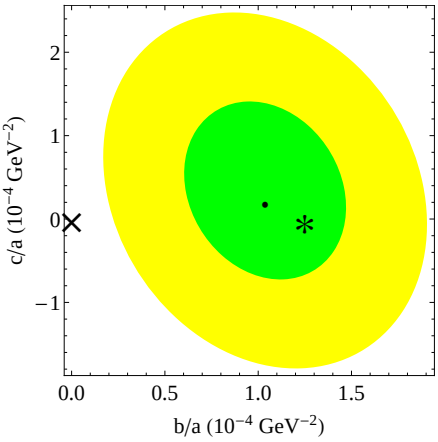

FIG. 11. c/a vs b/a 1σ (green) and 2σ (yellow) contours for Higgs with CP-even higher derivative contribution at 3000 fb^{-1}. The best fit value of $(b/a, c/a)$ is shown by the block dot. The values with which data are generated $(b/a = 1.25 \times 10^{-4}, c/a = 0)$ is shown by the '$*$'. The cross-hair corresponds to $b = c = 0$.

odd scenario we have taken $a = 0.75$, $b = 8 \times 10^{-5}$, $c = (1 + 1i) \times 10^{-4}$.

The values of the observables for CP-even higher derivative contribution are tabulated in Table VI. The

TABLE VI. The values of the observables for Higgs with CP-even higher derivative contribution and their respective errors at 3000 fb^{-1}.

Observables	**Values with errors**
t_2	-0.12 ± 0.04
t_1	$(0.31 \pm 3.40) \times 10^{-2}$
u_2	0.16 ± 0.18
u_1	$(-0.2 \pm 1.90) \times 10^{-1}$
v_2	$(-0.09 \pm 1.82) \times 10^{-1}$
v_1	$(-0.45 \pm 1.76) \times 10^{-1}$

best fit values for b/a and c/a with errors for CP-even higher derivative contribution are given as

$$b/a = (1.04 \pm 0.43) \times 10^{-4}\,\text{GeV}^{-2} \tag{41}$$

$$c/a = (0.34 \pm 1.07) \times 10^{-4}\,\text{GeV}^{-2} \tag{42}$$

The 1σ and 2σ contours for b/a vs c/a for Higgs with CP-even higher derivative contribution is shown in Fig. 11.

The values of observables for Higgs in CP-even-odd scenario are tabulated in Table VII. It should be noted that value of the observable t_1 is large due to non zero CP-odd admixture for the CP-even-odd scenario.

At 3000 fb^{-1} the best fit values of b/a, c/a, δ for the CP-even-odd scenario are given as

$$b/a = (0.59 \pm 0.40) \times 10^{-4}\,\text{GeV}^{-2} \tag{43}$$

$$c/a = (2.10 \pm 0.87) \times 10^{-4}\,\text{GeV}^{-2} \tag{44}$$

TABLE VII. The values of the observables for CP-even-odd scenario with respective errors at 3000 fb^{-1}.

Observables	**Values with errors**
t_2	-0.13 ± 0.04
t_1	0.02 ± 0.03
u_2	0.11 ± 0.18
u_1	$(0.27 \pm 1.89) \times 10^{-1}$
v_2	$(0.63 \pm 1.82) \times 10^{-1}$
v_1	$(0.83 \pm 1.78) \times 10^{-1}$

$$\delta = 0.57 \pm 1.33 \text{ in radian.} \tag{45}$$

The 1σ and 2σ contours for b/a vs c/a and δ vs c/a are shown in Fig. 12 and Fig. 13 respectively.

C. Momentum dependence of Higgs couplings

The vertex factors a, b and c written in Eq. (4) are in general momentum dependent but in SM they have no momentum dependence. Thus it is essential to verify their momentum independence to establish H as the SM Higgs. To achieve this, one has to measure the momentum dependence of a, b and c in different momentum regions. In LHC one only measures the ratios of couplings i.e. b/a and c/a. However one can measure the values of b/a and c/a in different $q_2^2(m_{34})$ regions. This will allow us to check the momentum dependence of b/a and c/a and finally a at 14 TeV 300 fb^{-1} LHC run.

Integrating Eq. (11), (12), (13) over q_2^2 we get uniangular distribution in n-th bin as follows

$$\frac{1}{\Gamma^n}\frac{d\Gamma}{d\cos\theta_1} = \frac{1}{2} - \mathcal{T}_1^n \cos\theta_1 + \mathcal{T}_2^n P_2(\cos\theta_1), \tag{46}$$

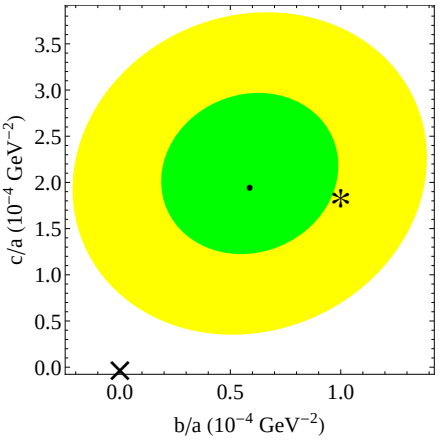

FIG. 12. c/a vs b/a 1σ (green) and 2σ (yellow) contours for CP-even-odd scenario Higgs at 3000 fb^{-1}. The best fit value of $(b/a, c/a)$ is shown by the block dot. The values with which data are generated ($b/a = 1.06 \times 10^{-4}$, $c/a = 1.89 \times 10^{-4}$) is shown by the '$*$'. The cross-hair corresponds to $b = c = 0$.

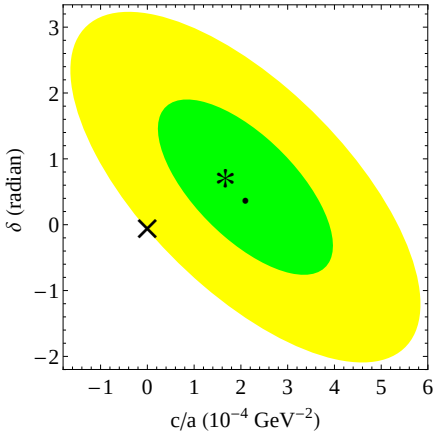

FIG. 13. δ vs c/a 1σ (green) and 2σ (yellow) contours for CP-even-odd scenario Higgs at 3000 fb^{-1}. The best fit values $(b/a, c/a)$ is shown by the block dot. The cross-hair corresponds to $\delta = c = 0$. The value with which data are generated is shown by the '$*$'.

$$\frac{1}{\Gamma^n}\frac{d\Gamma}{d\cos\theta_2} = \frac{1}{2} + \mathcal{T}_1^n \cos\theta_2 + \mathcal{T}_2^n P_2(\cos\theta_2), \tag{47}$$

$$\frac{1}{\Gamma^n}\frac{d\Gamma}{d\phi} = \frac{1}{2\pi} + \mathcal{U}_1^n \cos\phi + \mathcal{U}_2^n \cos 2\phi + \mathcal{V}_1^n \sin\phi + \mathcal{V}_2^n \sin 2\phi, \tag{48}$$

where $\mathcal{T}_1^n$, $\mathcal{T}_2^n$, $\mathcal{U}_1^n$, $\mathcal{U}_2^n$ $\mathcal{V}_2^n$ and $\mathcal{V}_1^n$ are observables in n-th bin integrated over q_2^2 range in that bin.

In SM the vertex factors are momentum independent and have constant values. This implies that a must have a constant value 1 and b, c should be zero in each m_{34} bin. As a result the values b/a, c/a will be zero in each m_{34} bin. In this subsection we bin the events and find the asymmetries $\mathcal{T}_1^n$, $\mathcal{T}_2^n$, $\mathcal{U}_1^n$, $\mathcal{U}_2^n$ and utilize them to find out b/a and c/a in three different bins.

Now we will study the momentum dependence of vertex factor 'a' in these 3 bins, we rewrite the decay width in n-th bin Γ_n as follows

$$\Gamma_n = a_n^2 \Gamma'_n\,(b/a, c/a)\,. \tag{49}$$

where a_n is the value of a in n-th bin. Γ'_n is obtained by dividing Γ_n by a^2 and making it a function of b/a and c/a only. We can calculate the values of Γ'_n and its errors in different bins by substituting the values of b/a and c/a from Table IX.

TABLE VIII. Three $\sqrt{q_2^2} = m_{34}$ bins and corresponding number of events in each bins for momentum dependence measurements at 14 TeV 300 fb^{-1} LHC run.

Bin No.	Bin range $\sqrt{q_2^2} = m_{34}$	Number of events
Bin 1	12.00 GeV $< m_{34} <$ 29.00 GeV	210
Bin 2	29.00 GeV $< m_{34} <$ 46.00 GeV	187
Bin 3	46.00 GeV $< m_{34} <$ 80.00 GeV	52

TABLE IX. b/a and c/a with corresponding errors in 3 bins in GeV^{-2}

Bin No.	b/a in 10^{-4}GeV^{-2}	c/a in 10^{-4}GeV^{-2}
Bin 1	0.02 ± 0.44	0.30 ± 0.57
Bin 2	0.39 ± 0.79	0.60 ± 0.89
Bin 3	1.35 ± 2.09	1.56 ± 2.24

Fit values of b/a and c/a have relatively larger errors in last bin due to small number of events and both b/a and c/a are consistent with zero in each m_{34} bins.

For resonant production of Higgs we can factor out the production cross-section and Γ_n is proportional to the number of events N_n in each of the three m_{34} bins. If Γ_i, Γ_j and N_i , N_j are the value of decay widths and number of events in i and j-th bin respectively, then

$$\frac{\Gamma_i}{\Gamma_j} = \frac{N_i}{N_j} \tag{50}$$

will hold between any two bins. Furthermore putting Γ_i and Γ_j expressions as written in Eq. (49) into Eq.(50) one finds the following relationship

$$r_{ij} = \frac{a_i}{a_j} = \sqrt{\frac{N_i}{N_j}\frac{\Gamma'_j}{\Gamma'_i}} \tag{51}$$

If a is independent of momentum the ratio r_{ij} will always be 1 for any two bins. We tabulate all possible r_{ij} in Table. X for this three bins with their corresponding errors. One can similarly perform the same analysis at 3000 fb^{-1}. At 3000 fb^{-1} the errors in b/a and c/a will be reduced and with the enhanced statistics, one may in principle have enough events to increase the number of bins to check momentum dependence of Higgs couplings.

TABLE X. Ratio r_{ij} between different bins.

Ratios (r_{ij})	values with errors
r_{12}	1.06 ± 0.28
r_{13}	0.82 ± 0.38
r_{23}	0.75 ± 0.39

These Ratios are consistent with SM (i.e ratio $r_{ij} = 1$) as they should. The ratio r_{13} and r_{23} have larger errors due to small statistics. These results will be improved by the bin size optimization and with larger statistics.

IV. COMPARISON OF PRECISION MEASUREMENT BETWEEN 33 TEV LHC AND ILC

After HL-LHC (High Luminosity LHC), LHC energy could be upgraded to run at a center of mass energy of $\sqrt{s} = 33$ TeV. In this section we compare the precision measurements of H coupling between 33 TeV LHC and ILC. We have followed the same cut based analysis as 14 TeV 3000 fb^{-1} machine. At 33 TeV 3000 fb^{-1} the number of events are given in the cut flow Table XI. The

Cuts	Number of events
Selection cuts	6523
50 GeV $< m_{12} <$ 106 GeV	6362
12 GeV $< m_{34} <$ 115 GeV	5935
115 GeV $< m_{4\ell} <$ 130 GeV	5852

TABLE XI. Effect of the sequential cuts on the simulated Signal for 33 TeV 3000 fb^{-1} LHC upgrade. The k-factor for signal is 1.95.

best fit values of b/a and c/a for SM Higgs are

$$b/a = (2.64 \pm 1.60) \times 10^{-5}\,\text{GeV}^{-2} \tag{52}$$

$$c/a = (1.07 \pm 6.25) \times 10^{-5}\,\text{GeV}^{-2} \tag{53}$$

In our first attempt, we find that a precision of 10^{-5} is achievable at the 33 TeV 3000 fb^{-1} LHC, for CP-odd admixture and CP-even higher derivative contribution. In future, a more detailed analysis may improve the result and decrease of errors in b/a and c/a. Although the precision achieved is high, LHC will only measure the ratios of Higgs couplings even at 33 TeV.

ILC will provide an independent test in measuring HZZ couplings subject to its proposed implementation and will also offer invaluable probe to such couplings. At LHC one measures $\sigma \cdot BR(H \to ZZ)$ however ILC will measure the branching ratio $BR(H \to ZZ)$ by measuring the inclusive cross section σ_{ZH} for the process $e^+e^- \to ZH$. This inclusive measurement of cross section alone will probe HZZ couplings to 1.3%[63]. Identifying a Z boson in recoil against the Higgs boson one

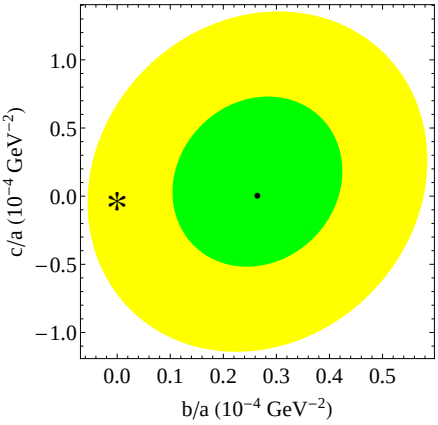

FIG. 14. c/a vs b/a 1σ (green) and 2σ (yellow) contours for SM Higgs at 33 TeV 3000 fb^{-1} LHC run. The best fit values $(b/a, c/a)$ is shown by the block dot. The '$*$' corresponds to $b = c = 0$.

can find out the partial width $\Gamma(H \to ZZ)$

$$\Gamma_{total} = \frac{\Gamma(H \to ZZ)}{BR(H \to ZZ)}. \tag{54}$$

For example the expected precision for CP-odd anomalous coupling c at ILC[64] is 7×10^{-4} to 8×10^{-6} which is roughly around the loop induced CP-odd contribution. We have shown that precision in the measurement of c/a can be 6×10^{-5} for 33 TeV LHC using angular asymmetries. However at ILC the measurement of Higgs decay width will allow us to extract the absolute values a, b, c which is beyond the scope of LHC.

V. CONCLUSION

We demonstrate that angular asymmetries will provide a strong and efficient tool to probe Higgs couplings in high luminosity future LHC runs. With the increased statistics at 14 TeV run, LHC will enter into precision era and angular analysis will offer a step by step methodology to study the Higgs couplings. Angular asymmetries can be utilized to probe the Higgs couplings and to disentangle its exact CP property in the next LHC run. We benchmark our observables for SM, CP-odd admixture, CP-even higher derivative contribution and finally CP-odd admixture with Higher derivative CP-even coupling. We perform the analysis for two different luminosities at 300 fb^{-1} as well as 3000 fb^{-1} and study the precision with which angular analysis probe HZZ couplings. The study of the momentum dependence of the Higgs couplings would be a significant step forward in establishing its SM nature, since in the SM Higgs couplings do not have any momentum dependence. At 14 TeV LHC run with the improved statistics, we present how one can examine the momentum dependence of the Higgs couplings in different momentum regions. We have further

discussed what precision LHC can achieve in the measurement of the Higgs couplings to Z boson by angular analysis at 33 TeV. A comparison has also been made between precision measurement of 33 TeV LHC and ILC. Angular analysis will be a powerful technique to decipher the CP properties of Higgs couplings at 14 TeV LHC run and will open up a new domain of precision measurement.

ACKNOWLEDGMENTS

Work of BB is supported by Department of Science and Technology, Government of INDIA under the Grant Agreement numbers IFA13-PH-75 (INSPIRE Faculty Award).

Appendix A

The amplitudes for the process H with spin $\mathbf{J}(spin\ 0)$ decays to two $Z(spin\ 1)$ boson with spin projections along z axis λ_1 and λ_2 is[67, 68]

$$\mathscr{M}(J_z,\lambda_1,\lambda_2)=\left(\frac{2J+1}{4\pi}\right)^{\frac{1}{2}}\mathscr{D}^{J*}_{J_z\lambda}(\Phi,\Theta,-\Phi)\,\mathcal{A}_{\lambda_1,\lambda_2}, \tag{A1}$$

where $\mathscr{D}^{J*}_{J_z\lambda}$ is the Wigner-D function, $\lambda=|\lambda_1-\lambda_2|$ and $\mathcal{A}_{\lambda_1,\lambda_2}$ are the *helicity amplitudes* with $\lambda_{1,2}\in\{\pm1,0\}$, $J=|\mathbf{J}|$. Angular momentum conservation implies $|\lambda|=|\lambda_1-\lambda_2|\leqslant J$ and the helicity amplitudes are related as $\mathcal{A}_{\lambda_2,\lambda_1}=(-1)^J\mathcal{A}_{-\lambda_1,-\lambda_2}$. We have three orthogonal helicity amplitudes $\mathcal{A}_{00}$, $\mathcal{A}_{++}$ and $\mathcal{A}_{--}$. However one can write three helicity amplitudes in transversity basis as:

$$\mathcal{A}_L=\mathcal{A}_{00} \tag{A2}$$

$$\mathcal{A}_\parallel=\frac{1}{\sqrt{2}}(\mathcal{A}_{++}+\mathcal{A}_{--}) \tag{A3}$$

$$\mathcal{A}_\perp=\frac{1}{\sqrt{2}}(\mathcal{A}_{++}+\mathcal{A}_{--}). \tag{A4}$$

Helicity fractions $\mathcal{F}_L$, $\mathcal{F}_\parallel$ and $\mathcal{F}_\perp$ are defined as $\mathcal{F}_\lambda=\dfrac{\mathcal{A}_\lambda}{\sqrt{|\mathcal{A}_L|^2+|\mathcal{A}_\parallel|^2+|\mathcal{A}_\perp|^2}}$, where $\lambda\in\{L,\parallel,\perp\}$.

Moreover $\eta=\frac{2v_\ell a_\ell}{v_\ell^2+a_\ell^2}$ with $v_\ell=2I_{3\ell}-4e_\ell\sin^2\theta_W$ and $a_\ell=2I_{3\ell}$.

$\Gamma_{\rm f}$ is defined as

$$\Gamma_{\rm f}=\frac{d\Gamma}{dq_2^2}=\mathcal{N}\left(|\mathcal{A}_L|^2+|\mathcal{A}_\parallel|^2+|\mathcal{A}_\perp|^2\right), \tag{A5}$$

with $\mathcal{N}=\frac{1}{2^4}\frac{1}{\pi^2}\frac{g^2}{\cos^2\theta_W}\frac{\mathrm{Br}^2_{\ell\ell}}{M_H^2}\frac{\Gamma_Z}{M_Z}\frac{X}{\left(\left(q_2^2-M_Z^2\right)^2+M_Z^2\Gamma_Z^2\right)}$. Γ_Z is the decay width of Z, $\mathrm{Br}_{\ell\ell}$ is the branching fraction for the decay of Z to two massless leptons. However we assumed narrow width approximation for on-shell Z_1 boson in Sec.II. In Sec.III we have implemented the the cut flow table while integrating over q_1^2 and q_2^2 to find the expressions for $\mathcal{T}_1$, $\mathcal{T}_2$, $\mathcal{U}_1$, $\mathcal{U}_2$, $\mathcal{V}_1$ and $\mathcal{V}_2$.

The expressions for $\mathcal{T}_1$, $\mathcal{T}_2$, $\mathcal{U}_1$, $\mathcal{U}_2$, $\mathcal{V}_1$ and $\mathcal{V}_2$ are

$$\mathcal{T}_1=\frac{1.32\times10^{-9}y}{5.57\times10^{-8}+2.61\times10^{-8}x+3.98\times10^{-9}x^2+1.60\times10^{-10}y^2} \tag{A6}$$

$$\mathcal{T}_2=\frac{-9.65\times10^{-9}+4.00\times10^{-10}x^2+4.00\times10^{-10}y^2}{5.57\times10^{-8}+2.61\times10^{-8}x+3.98\times10^{-9}x^2+1.60\times10^{-10}y^2} \tag{A7}$$

$$\mathcal{U}_1=\frac{-1.20\times10^{-9}-6.33\times10^{-10}x+7.11\times10^{-11}x^2}{5.57\times10^{-8}+2.61\times10^{-8}x+3.98\times10^{-9}x^2+1.60\times10^{-10}y^2} \tag{A8}$$

$$\mathcal{U}_2=\frac{6.06\times10^{-9}+4.35\times10^{-9}x+7.97\times10^{-10}x^2+4.00\times10^{-10}y^2}{5.57\times10^{-8}+2.61\times10^{-8}x+3.98\times10^{-9}x^2+1.60\times10^{-10}y^2} \tag{A9}$$

$$\mathcal{V}_1=\frac{3.11\times10^{-10}y}{5.57\times10^{-8}+2.61\times10^{-8}x+3.98\times10^{-9}x^2+1.60\times10^{-10}y^2} \tag{A10}$$

$$\mathcal{V}_2=\frac{-2.92\times10^{-9}y}{5.57\times10^{-8}+2.61\times10^{-8}x+3.98\times10^{-9}x^2+1.60\times10^{-10}y^2} \tag{A11}$$

where $x=\frac{b}{a}\times(100\mathrm{Gev})^2$ and $y=\frac{c}{a}\times(100\mathrm{Gev})^2$

[1] G. Aad *et al.* [ATLAS Collaboration], Phys. Lett. B **716**, 1 (2012) [arXiv:1207.7214 [hep-ex]].

[2] G. Aad *et al.* [ATLAS Collaboration], Science 21 Decem-

ber 2012: Vol. 338 no. 6114 pp. 1576-1582.
[3] S. Chatrchyan *et al.* [CMS Collaboration], Phys. Lett. B **716**, 30 (2012) [arXiv:1207.7235 [hep-ex]].
[4] S. Chatrchyan *et al.* [CMS Collaboration], Science 21 December 2012: Vol. 338 no. 6114 pp. 1569-1575.
[5] S. Chatrchyan *et al.* [CMS Collaboration], arXiv:1212.6639 [hep-ex].
[6] C. A. Nelson, Phys. Rev. D **30**, 1937 (1984).
[7] J. R. Dell'Aquila and C. A. Nelson, Phys. Rev. D **33**, 80 (1986).
[8] C. A. Nelson, Pair)," Phys. Rev. D **37**, 1220 (1988).
[9] M. Kramer, J. H. Kuhn, M. L. Stong and P. M. Zerwas, Z. Phys. C **64**, 21 (1994) [hep-ph/9404280].
[10] V. D. Barger, K. -M. Cheung, A. Djouadi, B. A. Kniehl and P. M. Zerwas, Phys. Rev. D **49**, 79 (1994) [hep-ph/9306270].
[11] J. F. Gunion and X. -G. He, Phys. Rev. Lett. **76**, 4468 (1996) [hep-ph/9602226].
[12] D. J. Miller, S. Y. Choi, B. Eberle, M. M. Muhlleitner and P. M. Zerwas, Phys. Lett. B **505**, 149 (2001) [hep-ph/0102023].
[13] G. R. Bower, T. Pierzchala, Z. Was and M. Worek, Phys. Lett. B **543**, 227 (2002) [hep-ph/0204292].
[14] S. Y. Choi, "Measuring the spin of the Higgs bosons,"in 10th International Conference on Supersymmetry, Edited by P. Nath, P. M. Zerwas, C. Grosche. Hamburg, DESY, 2002.
[15] S. Y. Choi, D. J. Miller, M. M. Muhlleitner and P. M. Zerwas, Phys. Lett. B **553**, 61 (2003) [hep-ph/0210077].
[16] R. M. Godbole, S. D. Rindani and R. K. Singh, Phys. Rev. D **67**, 095009 (2003) [Erratum-ibid. D **71**, 039902 (2005)] [hep-ph/0211136].
[17] C. P. Buszello, I. Fleck, P. Marquard and J. J. van der Bij, Eur. Phys. J. C **32**, 209 (2004) [hep-ph/0212396].
[18] K. Desch, Z. Was and M. Worek, Eur. Phys. J. C **29**, 491 (2003) [hep-ph/0302046].
[19] M. Worek, Acta Phys. Polon. B **34**, 4549 (2003) [hep-ph/0305082].
[20] A. B. Kaidalov, V. A. Khoze, A. D. Martin and M. G. Ryskin, Eur. Phys. J. C **31**, 387 (2003) [hep-ph/0307064].
[21] R. M. Godbole, S. Kraml, M. Krawczyk, D. J. Miller, P. Niezurawski and A. F. Zarnecki, hep-ph/0404024.
[22] C. P. Buszello and P. Marquard, hep-ph/0603209.
[23] H. Przysiezniak, hep-ex/0605069.
[24] M. Bluj, CMS-NOTE-2006-094.
[25] P. S. Bhupal Dev, A. Djouadi, R. M. Godbole, M. M. Muhlleitner and S. D. Rindani, Phys. Rev. Lett. **100**, 051801 (2008) [arXiv:0707.2878 [hep-ph]].
[26] R. M. Godbole, D. J. Miller, 2 and M. M. Muhlleitner, JHEP **0712**, 031 (2007) [arXiv:0708.0458 [hep-ph]].
[27] R. M. Godbole, P. S. Bhupal Dev, A. Djouadi, M. M. Muhlleitner and S. D. Rindani, eConf C **0705302**, TOP08 (2007) [arXiv:0710.2669 [hep-ph]].
[28] Y. Gao, A. V. Gritsan, Z. Guo, K. Melnikov, M. Schulze and N. V. Tran, Phys. Rev. D **81**, 075022 (2010) [arXiv:1001.3396 [hep-ph]].
[29] C. Englert, C. Hackstein and M. Spannowsky, Phys. Rev. D **82**, 114024 (2010) [arXiv:1010.0676 [hep-ph]].
[30] O. J. P. Eboli, C. S. Fong, J. Gonzalez-Fraile and M. C. Gonzalez-Garcia, Phys. Rev. D **83**, 095014 (2011) [arXiv:1102.3429 [hep-ph]].
[31] U. De Sanctis, M. Fabbrichesi and A. Tonero, Phys. Rev. D **84**, 015013 (2011) [arXiv:1103.1973 [hep-ph]].
[32] S. Berge, W. Bernreuther, B. Niepelt and H. Spiesberger, Phys. Rev. D **84**, 116003 (2011) [arXiv:1108.0670 [hep-ph]].
[33] M. C. Kumar, P. Mathews, A. A. Pankov, N. Paver, V. Ravindran and A. V. Tsytrinov, Phys. Rev. D **84**, 115008 (2011) [arXiv:1108.3764 [hep-ph]].
[34] J. Ellis and D. S. Hwang, JHEP **1209**, 071 (2012) [arXiv:1202.6660 [hep-ph]].
[35] C. Englert, M. Spannowsky and M. Takeuchi, JHEP **1206**, 108 (2012) [arXiv:1203.5788 [hep-ph]].
[36] A. Bredenstein, A. Denner, S. Dittmaier and M. M. Weber, Phys. Rev. D **74**, 013004 (2006) [hep-ph/0604011].
[37] J. Ellis, D. S. Hwang, V. Sanz and T. You, arXiv:1208.6002 [hep-ph].
[38] J. Ellis, R. Fok, D. S. Hwang, V. Sanz and T. You, arXiv:1210.5229 [hep-ph].
[39] P. P. Giardino, K. Kannike, M. Raidal and A. Strumia, arXiv:1207.1347 [hep-ph].
[40] S. Y. Choi, M. M. Muhlleitner and P. M. Zerwas, arXiv:1209.5268 [hep-ph].
[41] R. Boughezal, T. J. LeCompte and F. Petriello, arXiv:1208.4311 [hep-ph].
[42] S. Banerjee, J. Kalinowski, W. Kotlarski, T. Przedzinski and Z. Was, arXiv:1212.2873 [hep-ph].
[43] P. Avery, D. Bourilkov, M. Chen, T. Cheng, A. Drozdetskiy, J. S. Gainer, A. Korytov and K. T. Matchev *et al.*, arXiv:1210.0896 [hep-ph].
[44] B. Coleppa, K. Kumar and H. E. Logan, Phys. Rev. D **86**, 075022 (2012) [arXiv:1208.2692 [hep-ph]].
[45] C. -Q. Geng, D. Huang, Y. Tang and Y. -L. Wu, arXiv:1210.5103 [hep-ph].
[46] J. Ellis, V. Sanz and T. You, arXiv:1211.3068 [hep-ph].
[47] J. Frank, M. Rauch and D. Zeppenfeld, arXiv:1211.3658 [hep-ph].
[48] A. Djouadi, R.M. Godbole, B. Mellado and K. Mohan arXiv:1301.4965 [hep-ph].
[49] C. Englert, D. Goncalves-Netto, K. Mawatari and T. Plehn, arXiv:1212.0843 [hep-ph].
[50] D. Stolarski and R. Vega-Morales, Bosons," Phys. Rev. D **86**, 117504 (2012) [arXiv:1208.4840 [hep-ph]].
[51] J. S. Gainer, J. Lykken, K. T. Matchev, S. Mrenna and M. Park, Phys. Rev. Lett. **111**, 041801 (2013) [arXiv:1304.4936 [hep-ph]].
[52] M. Chen, T. Cheng, J. S. Gainer, A. Korytov, K. T. Matchev, P. Milenovic, G. Mitselmakher and M. Park *et al.*, Phys. Rev. D **89**, no. 3, 034002 (2014) [arXiv:1310.1397 [hep-ph]].
[53] A. Menon, T. Modak, D. Sahoo, R. Sinha and H. Y. Cheng, Phys. Rev. D **89**, 095021 (2014) [arXiv:1301.5404 [hep-ph]].
[54] ATLAS Collaboration, Prospects for measurements of the HZZ vertex tensor structure in H $\to$ ZZ* $\to$ 4l decay channel with ATLAS ATLAS-PHYS-PUB-2013-013
[55] V. Khachatryan *et al.* [CMS Collaboration], arXiv:1411.3441 [hep-ex].
[56] I. Anderson, S. Bolognesi, F. Caola, Y. Gao, A. V. Gritsan, C. B. Martin, K. Melnikov and M. Schulze *et al.*, Phys. Rev. D **89**, no. 3, 035007 (2014) [arXiv:1309.4819 [hep-ph]].
[57] T. Modak and R. Srivastava, arXiv:1411.2210 [hep-ph].
[58] N. Belyaev, R. Konoplich, L. E. Pedersen and K. Prokofiev, arXiv:1502.03045 [hep-ph].
[59] Y. Chen, R. Harnik and R. Vega-Morales, arXiv:1503.05855 [hep-ph].

[60] G. Buchalla, O. Cata and G. D'Ambrosio, Eur. Phys. J. C **74**, 2798 (2014) [arXiv:1310.2574 [hep-ph]].

[61] M. Beneke, D. Boito and Y. M. Wang, arXiv:1406.1361 [hep-ph].

[62] T. Modak, D. Sahoo, R. Sinha, H. Y. Cheng and T. C. Yuan, arXiv:1408.5665 [hep-ph].

[63] H. Baer, T. Barklow, K. Fujii, Y. Gao, A. Hoang, S. Kanemura, J. List and H. E. Logan *et al.*, arXiv:1306.6352 [hep-ph].

[64] D. M. Asner, T. Barklow, C. Calancha, K. Fujii, N. Graf, H. E. Haber, A. Ishikawa and S. Kanemura *et al.*, arXiv:1310.0763 [hep-ph].

[65] L. D. Landau, Dokl. Akad. Nauk Ser. Fiz. **60**, 207 (1948).

[66] C. -N. Yang, Phys. Rev. **77**, 242 (1950).

[67] M. Jacob and G. C. Wick, Annals Phys. **7**, 404 (1959) [Annals Phys. **281**, 774 (2000)].

[68] Suh-Urk Chung, "Spin formalisms, Updated Version", Brookhaven Nat. Lab., Upton, NY, 2008. This report is an updated version of CERN-71-08.

[69] Wolfram Research, Inc., Mathematica, Version 9, Champaign, IL.

[70] G. Aad *et al.* [ATLAS Collaboration], Phys. Lett. B **726**, 120 (2013) [arXiv:1307.1432 [hep-ex]].

[71] ATLAS Collaboration, decay channel with the ATLAS detector using 25 fb?1 of proton-proton collision data" ATLAS-CONF-2013-029

[72] CMS Collaboration, "Measurements of the properties of the Higgs-like boson in the four lepton decay channel with the ATLAS detector using 25 fb?1 of proton-proton collision data" CMS PAS HIG-13-002

[73] ATLAS Collaboration, "Measurements of the properties of the Higgs-like boson in the four lepton decay channel with the ATLAS detector using 25 fb?1 of proton-proton collision data"ATLAS-CONF-2013-013

[74] J. Pumplin, D. R. Stump, J. Huston, H. L. Lai, P. M. Nadolsky and W. K. Tung, JHEP **0207**, 012 (2002) [arXiv:hep-ph/0201195].

[75] J. Alwall, M. Herquet, F. Maltoni, O. Mattelaer and T. Stelzer, JHEP **1106** (2011) 128 [arXiv:1106.0522 [hep-ph]].

[76] T. Sjostrand, L. Lonnblad, S. Mrenna and P. Z. Skands, hep-ph/0308153.

[77] J. de Favereau *et al.* [DELPHES 3 Collaboration], JHEP **1402**, 057 (2014) [arXiv:1307.6346 [hep-ex]].

[78] P. Artoisenet, P. de Aquino, F. Demartin, R. Frederix, S. Frixione, F. Maltoni, M. K. Mandal and P. Mathews *et al.*, JHEP **1311**, 043 (2013) [arXiv:1306.6464 [hep-ph]].

[79] Webpage for Higgs cross sections at 7, 8 and 14 TeV (LHC Higgs Cross Section Working Group)